Available online at www.sciencedirect.com

jmr&t Journal of Materials Research and Technology

journal homepage: www.elsevier.com/locate/jmrt

Original Article

Influence of temperature on the electrochemical coloration process and properties of the AISI 304 and 430 colored stainless steel

J.L. Silva [a,*], Andreia Rocha Canella Carneiro [b], Geovane Martins Castro [c], Eduardo Henrique Martins Nunes [d], Vanessa de Freitas Cunha Lins [a], Rosa Maria Rabelo Junqueira [a]

[a] Department of Chemical Engineering, Federal University of Minas Gerais, Av. Antônio Carlos 6627, 31279-901, Belo Horizonte, Minas Gerais, Brazil
[b] Redemat/Federal University of Ouro Preto, Minas Gerais, Brazil
[c] Research Center, Aperam South America, Timóteo, Minas Gerais, Brazil
[d] Department of Metallurgical and Materials Engineering, Federal University of Minas Gerais, Brazil

ARTICLE INFO

Article history:
Received 29 September 2021
Accepted 23 November 2021
Available online 1 December 2021

Keywords:
Colored stainless steel
Nanoindentation
Wettability
Interference film
Nanohardness

ABSTRACT

The influence of temperature on the speed of an electrochemical coloration process of AISI 304 and AISI 430 stainless steel was investigated in temperature ranging from 25 °C to 40 °C. The surface properties of the interference colored nanofilms obtained in both types of stainless steel substrates, were also evaluated. A higher coloring speed was observed for AISI 304. The coloring time to obtain a gold color decreased with increasing temperature for both steels. This effect was stronger on the AISI 430 substrate, with a decrease of 36.6% in the coloration time for the samples colored at 40 °C and 25 °C. The Arrhenius model was applied to estimate the equations of colored films growth rate. The films porous fractions evaluated by SEM were in the range of 27–29%, without relevant variation with the coloring temperature. The nanohardness of the conjugated film-substrate obtained in a nano-indenter coupled to an AFM shows lower values than the uncolored substrates, and this reduction is more significant for the films grown on the AISI 430 ferritic specimens. The wettability of the surface to water and oil increased after coloring. The amplification effect of the hydrophilic effect can be associated with the increased AFM nanorugosity values.

1. Introduction

The colored SS is visually impacting for use as coatings, appliances and others applications that demand design differentiated. A wide variety of interference colors can be obtained according to the thickness of the film, including brown, blue, gold, purple and green, in this sequence, with the increase of tenths of nanometers to approximately half a

* Corresponding author.
E-mail address: jaquelinelacerdaj@gmail.com (J.L. Silva).
https://doi.org/10.1016/j.jmrt.2021.11.117

Table 1 – Chemical composition of samples (% by mass).

Steel	C	Mn	Si	S	Cr	Ni	Nb	Mo	Ti	W
AISI 430	0.047	0.178	0.277	0.0003	16.1	0.137	0.005	0.006	0.003	0.004
AISI 304	0.037	1.149	0.456	0.0010	17.7	8.022	0.012	0.124	0.003	0.024

Source: Certificates of analysis provided by APERAM South America.

micrometer thick. In addition to the aesthetic factor conferred to the steel by the surface color resulting from the interference of light reflected at the interfaces of the oxide/air film and steel/oxide film, several studies showed the excellent corrosion resistance of the interference film, because of its anodic protection [1–3].

The first process known applied to coloring the SS was by chemical oxidation under high temperature, generating an amount of acid vapors and poor color reproducibility [4]. Electrochemical methods using square wave potential pulse polarization or alternating pulse current in sulfochromic solution were later developed, allowing to work in milder conditions, with greater color reproducibility and operational control [2,3,5,6].

The knowledge of the growth rate of nanofilms on different substrates and of the effect of the temperature on the growth rate of coloring films enables productivity improving of the electrochemical coloring process of SS. In the studies by Wang and Duh [7], they evaluated the effect of temperature on the alternating current pulse coloring process in AISI 304 stainless steel. Temperatures of 65, 72 and 80 °C were used. The coloring times expressed in alternating potentiometric cycles applied decreased faster as the temperature increases. Junqueira et al. [8] studied the morphology of the interference films grown using alternating pulse current process on AISI 304 substrate in low chromium concentration at different temperatures, and evaluated the surface roughness, abrasion resistance and hardness of the films. The works [7,8] did not evaluate the growth rate of the films.

Arrhenius suggested dependence of the specific reaction rate, k, with the temperature:

$$k_A(T) = A\exp^{-E/RT} \quad (1)$$

where, A is pre-exponential factor or frequency factor, E is the activation energy, J/mol or cal/mol, R is the universal gas constant, and T is the absolute temperature in Kelvin (K). Equation (1) is known as the Arrhenius equation and has been empirically proven as the strong dependence of the constant k to temperature. In many cases, the observed rate of a chemical reaction increases as the temperature is raised, but the extent of this growth varies greatly from reaction to reaction [9].

Many studies have focused on the study of the electrochemical coloring process and its influence on the properties of austenitic SS, such as AISI 304 [1–8]. The AISI 430 ferritic SS, despite its commercial appeal due to its low nickel concentration, presents few studies for electrochemical coloration its surface. A study was carried out with AISI 430 steel using electrochemical and photochemical steps with a sulfochromic solution for coloring. The process occurs in open circuit potential and under visible light illumination, yielding a golden color interference film about 2 h after the beginning of the coloring process [10].

A very interesting characteristic of SS is the achievement of easy-to-clean or anti-fingerprint surfaces and has been the subject of many studies using coating deposition with several different methods [11–13]. Therefore, several wettability studies to increase hydrophobicity and oleophobicity were carried out with the SS, but none refer the wettability caused by interference films grown on the SS surface by electrochemical processes. A superhydrophobic colored surface on AISI 304 stainless steel substrate was obtained by performing a chemical attack to increase the surface roughness, followed by a chemical oxidation coloring process at 80 °C. Later the colored surface was coated and modified with PFOTES (1H, 1H,2H,2H-Perfluorooctyltriethoxysilane) by solution-immersion. After coloring by chemical oxidation, hydrophilic surfaces were obtained, allowing the generation of a superhydrophobic surface after modification with PFOTES, with contact angles with water up to 152° [11].

In addition to chemical composition, wettability is also related to the roughness and porosity of a surface. The increase of the surface roughness accentuates its hydrophilic or hydrophobic character [14,15]. The same relationship is valid when evaluating porosity, since roughness can be perceived as a surface porosity where air is trapped, forming a composite air/solid material surface [16].

In this context, this study evaluated the influence of temperature on coloring time, describing the Arrhenius equation on ferritic and austenitic SS substrates, as well as the influence of temperature and substrate on the porosity, nanoroughness, nanohardness and wettability in water and oil of interference films generated, using an electrochemical patented process of pulsed current coloring [17].

To the best of our knowledge, the literature is very scarce on the wettability study of colored stainless steel, on the evaluation of the effect of temperature on the growth rate of the interference colored anodic film, grown on ferritic and austenitic stainless steel. There is a gap in the literature about the coloration of a ferritic SS, which is an innovative aspect of the present work.

2. Experimental

2.1. *Preparation of stainless steel samples*

Samples of AISI 304 austenitic SS and AISI 430 ferritic SS, 0.8 mm thick, Buffing Bright (BB) finish. The samples were cut in pieces of 60 mm × 50 mm, degreased with petroleum ether, washed with detergent and water, and dried with air jet. Table 1 shows the chemical composition of the steels.

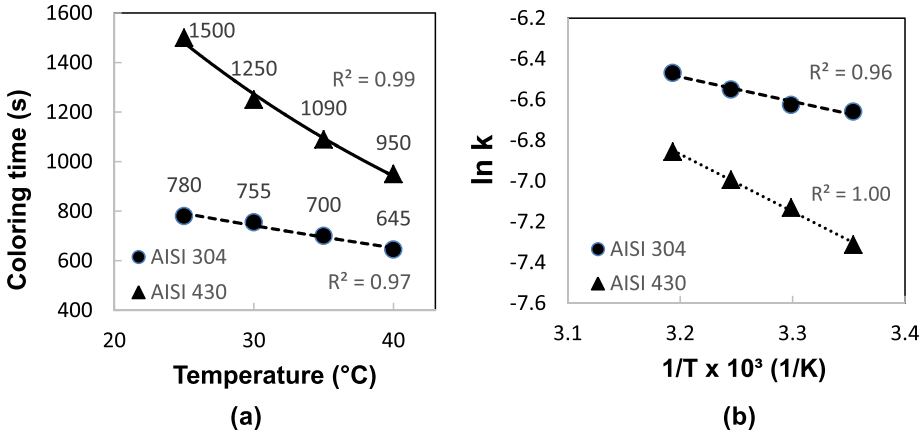

Fig. 1 – (a) Coloring time depending on the temperature of the solution and (b) Arrhenius graph for the growth rate of the interference film versus the reciprocal of the temperature.

2.2. *Coloration*

The samples were colored according to the procedure patented by CETEC [17], with anodic pretreatment in 10% sodium sulfate solution (wt/v) and alternating current of 0.85 A/dm^2, subsequently colored in sulfochromic solution 2.5 M CrO_3/5.0 M H_2SO_4 and current of 0.12 A/dm^2, with pulse size of 4/1, using an Ivium Compactstat potentiostat. A cathodic hardening treatment was performed with chromic acid solution in water (500 g CrO_3/l) for 10 min, with a current density of 0.5 A/dm^2 in a Minipa MPL1303M DC power supply. The coloring process was performed at temperatures of 25, 30, 35, and 40 °C in a thermostated water bath.

The postulate of the Arrhenius equation enables the experimental determination of the activation energy leading to a reaction at different temperatures. After applying the natural logarithm (ln) to Equation (1), we obtain Equation (2):

$$\ln k_A = \ln A - \frac{E}{R}\left(\frac{1}{T}\right) \quad (2)$$

From the Equation (2) was possible to extract the activation energy (E) by calculating the angular coefficient obtained when plotting ln k_A as a function of 1/T. With the knowledge of the specific reaction rate (k) at a given temperature (T_0), and the activation energy, we can determine the value of k at any other temperature, T [9].

The coloring time was recorded in order to reach the golden color in all samples. The rate of the coloring process was calculated considering a constant film thickness for the golden color, and the specific reaction rate constant, k, using a constant value C (nm) to the coloring time in seconds.

2.3. *Characterization of films*

2.3.1. *Color and brightness*

Color measurements were performed in a BYK Gardner Spectro-Guide Sphere Spectrophotometer. The color scale used was CIE LCh*, where L is luminosity (white-black), C is saturation (pale-vivid) and h* is color hue (green, red, blue, yellow). The brightness was determined using a BYK Gardner Tri-gloss brightness meter using a D65 light source and a 10° standard observer.

Four samples were prepared in each temperature condition and five measurements were performed for each sample.

2.3.2. *Nanoporosity*

Morphological characteristics of the colored SS were evaluated using the Scanning Electron Microscope (SEM) - FEI Quanta 3D FEG. For the evaluation of the porosity of the samples, acceleration potentials between 3 and 5 kV were used, with magnification in the range of 20 000 to 200 000 x. The porous fraction and pore size were obtained by image processing using ImageJ software [18].

2.3.3. *Nanoroughness and nanoindentation*

Nanoroughness and nanoindentation assays were performed under an Atomic Force Microscope (AFM) MFP-3D-SA ASYLUM RESEARCH. The scanning area was 400 μm^2 (20 μm × 20 μm), using the intermittent contact mode and C-160 TS probe of 9 ± 2 nm of radius silicon, with a reading of 256 points and peak amplitude of 1 V. The instrumented nanoindentation test (IIT) were performed from a nanoindenter coupled to the AFM. The Force-Displacement curves were raised to determine nanohardness and modulus of elasticity using a 2 mN load, with a loading cycle of 10 s, 5 s of load permanence, and another 10 s of discharge. Berkovith triangular pyramid with Poisson coefficient of 0.33 was used as indenter. Six replicates were analyzed in each test.

2.3.4. *Wettability in water and oil*

The hydrophobicity and oleophobicity of the samples were quantified by contact angle measurements, performed at room temperature, using deionized water and ultrapure mineral oil (Nujol Mantecorp), respectively. The measurements were performed using a Digidrop goniometer – DI, GBX Instruments with a camera attached. The Visiodrop software was used for image analysis. The deposited volume of deionized water and ultrapure mineral oil droplets were 3 μL.

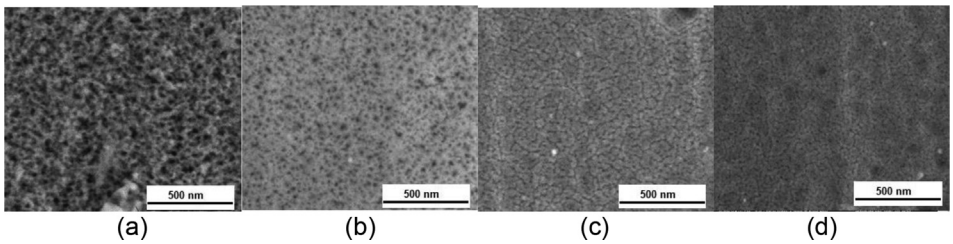

Fig. 2 – Typical SEM Images of SS colored in gold by an electrochemical process at different temperatures, being (a) AISI 430 25 °C, (b) AISI 430 40 °C, (c) AISI 304 25 °C, (d) AISI 304 40 °C.

Averages obtained from 13 measurements in 5 different images.

2.4. *Statistical analysis*

The ANOVA analysis was adopted for design with a 95% confidence interval (alpha = 0.05), using the Tukey test to evaluate honestly significant differences, calculated by Past [19] software. The comparative characterization tests were performed with statistically equal samples of the color hue (h) parameter, assuming identical layer thicknesses for the colored samples.

3. Results and discussion

3.1. *Rate of the coloring process*

The growth of the interference film was controlled by the time applied during the coloring step. The golden coloring of the AISI 304 and AISI 430 was obtained at temperatures of 25 °C, 30 °C, 35 °C and 40 °C.

The coloring process of AISI 304 was faster than the AISI 430 SS, since, to obtain the same golden coloration at 25 °C, AISI 304 required 780 s, while for AISI 430, it took 1500 s, almost twice the time. The related samples data for coloring temperature, as well as the results of the color and brightness analyses were used to build the graph illustrated in Fig. 1(a). It was observed an exponential reduction of coloring time with the increase of temperature for AISI 304 and 430. The AISI 430 showed a higher influence of temperature on its interference film growth rate, with a reduction of 36.6% in coloring time ranging from 25 °C to 40 °C, while for AISI 304 the reduction was 17.3% for the same temperature range.

In an attempt to investigate the rate of steel coloration, the activation energy and the frequency factor were estimated by linearizing the data obtained experimentally at the temperatures studied, from the Equations (1) and (2). With the equations of the linearized lines as shown in Fig. 1(b), we obtained activation energy of 9999 J/mol for the SS AISI 304 and 23 419 J/mol for AISI 430, showing that the latter is more sensitive to temperature variations. Reactions with high activation energies are more sensitive to temperature variations. From the experimental results, it was possible to estimate the specific growth rates of the films by the Arrhenius model:

$$k_{(T)ABNT\ 304} = 0.071 * e^{\frac{-9.999}{RT}} \quad (3)$$

$$k_{(T)ABNT\ 430} = 8.585 * e^{\frac{-23.419}{RT}} \quad (4)$$

A less noble metal under the point of corrosion resistance, as is the case of ferritic AISI 430 SS, the anodic and cathodic reactions in a highly oxidizing solution should occur faster, accelerating the process of obtaining the interference film, but what occurs in the coloring process did not demonstrate this behavior. We observed that a shorter time to obtain the same coloring condition was obtained for AISI 304.

3.2. *Characterization of interference films*

3.2.1. *Porosity*

The porosity of interference films are showed in Fig. 2. The films grown on the AISI 304 SS are compacted, with smaller pores, apparently interconnected. On the surface of films grown on the AISI 430, the pore distribution is homogeneous, apparently not so compacted, with independent, larger and regular pores.

In Table 2, the results show no variability among the colored samples on different substrates and different temperatures, when evaluating the porous area fraction, ranging between a porous area of 27%–28%.

The pore size did not present significant variability influenced by the temperature of the coloring process, but differed to the type of steel, presenting larger pores for AISI 430 steel, confirming the observations made in the images. Using the transmission electronic microscopic (TEM) technique, Evans

Table 2 – Porous area and pore diameter of colored samples at 25 °C and 40 °C.

		AISI 304 25 °C	AISI 304 40 °C	AISI 430 25 °C	AISI 430 40 °C
Porous Area (%) Fraction	Average (%)	27.02 ± 0.35 [(a)]	27.60 ± 0.91 [(a)]	28.64 ± 0.55 [(a)]	28.83 ± 0.98 [(a)]
Pore Diameter (nm)	Average (nm)	16.63 ± 3.79 [(b)]	14.92 ± 3.93 [(b)]	22.83 ± 3.66 [(c)]	22.88 ± 3.83 [(c)]

Note: Averages that share the same letter are significantly similar by the Tukey test. Porous fraction: Averages obtained from 10 measurements in 3 different images (30 measurements). Pore diameter: Average obtained of 12 measurements.

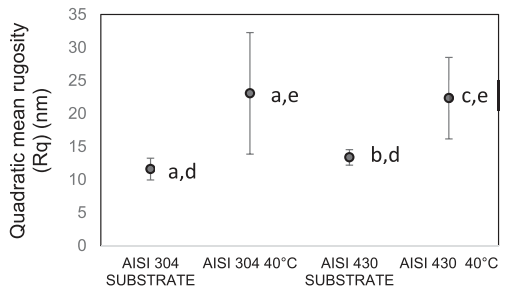

Fig. 3 – Quadratic mean roughness (Rq) of SS substrates and color samples at 40 °C. The average values that share the same letter are significantly similar according to the statistic Tukey test.

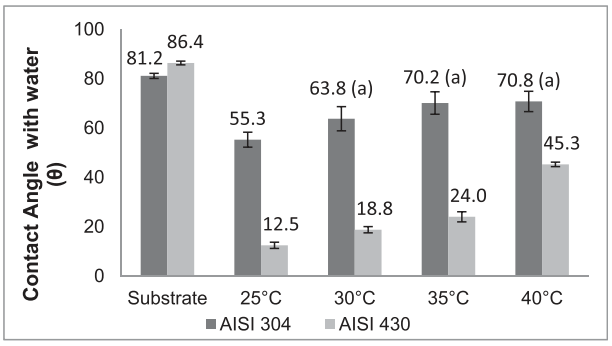

Fig. 5 – Mean values of the contact angle of the samples for evaluation of water wettability. Values that share the same letter are significantly similar according to the statistic Tukey test.

[4] identified a porous fraction of 20–30% in the films colored by chemical process on a SS AISI 304 substrate, which agrees with the results obtained in this study.

3.2.2. *Nanoroughness*

The nanoroughness values expressed in mean quadratic roughness (Rq) are shown in Fig. 3. An increase of the nanoroughness of the samples after coloring occurred for the two substrates. The nanoroughness of AISI 430 increased after the coloring process while no significant difference was observed for the AISI 304 colored at 40 °C compared with the bare substrate. Considering the tested hypothesis there is no difference in the nanoroughness of the two substrates.

Junqueira et al. [6] evaluated the effect of the scan size on the Rq of the AISI 304 substrate and with interference film. The values found for scanning 20 μm × 20 μm were 11.09 nm for the substrate and approximately 15 nm for the color film, values of the same order of magnitude as those found in this study.

3.2.3. *Nanoindentation*

The force–displacement curves represented in Fig. 4 were obtained in instrumented indentation tests of AISI 304 and 430 SS before and after coloration at 25 °C. A higher penetration depth for the 2 mN applied force is observed for the colored AISI 430, and lower resistance to deformation when compared to its substrate. The profiles of the deformation curves of AISI 430 SS, both of the samples with the interference film and of the substrate, are similar, with partially reversible deformation (elastic) after the force being discharged. Similar behavior was observed for the other samples analyzed in the IIT.

Table 3 shows the measurements obtained in IIT of the surface of substrates and conjugated interference-substrate films, applying a load of 2 mN through a nanoindentator coupled to the AFM. The substrates showed a higher modulus of elasticity, with a reduction of the same parameter in the colored samples. Ferritic SS has a smaller modulus of elasticity for both the substrate and the film–substrate conjugate. The higher the modulus of elasticity, the stiffer the material and the smaller its elastic deformation [20]. A higher penetration depth of 2 mN applied force is observed for AISI 430 colored at 25 °C, presenting a lower resistance to deformation when compared to its substrate. For all mechanical properties evaluated, both substrates were statistically identical.

The results of maximum penetration depth for the samples after the coloring processes are superior to the substrates, and the interference films were grown on the ferritic substrate present higher penetration. These results are in accordance with the values obtained of nanohardness, resulting in the reduction of this after coloring, and this reduction is more significant for the films on the ferritic substrate, which makes the interference films less resistant to localized plastic deformation.

As discussed earlier, the interference film on the AISI 430 substrate has larger pores, a relevant factor in the hardness of the film. It is not possible to evaluate the significant difference in the nanomechanical parameters measured by varying the temperature of the coloring process. Due to the limitations of the equipment, the applied force of 2 mN caused a penetration greater than 10% of the thickness of the interference film, and

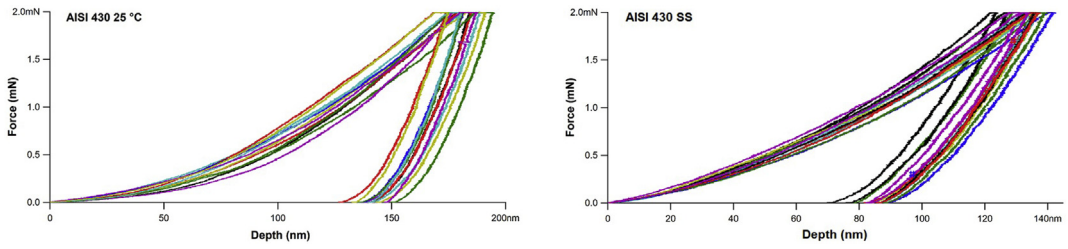

Fig. 4 – Typical displacement–force curves of AISI 430 SS colored at 25 °C and of AISI 430 SS, obtained by instrumented indentation tests in AFM.

Table 3 – Nanomechanical parameters obtained by instrumented indentation by using AFM of substrates and colored steels. Values that share the same letter are significantly similar according to the statistic Tukey test.

	Elastic modulus (GPa)	Indentation Depth (nm)	Nanohardness (GPa)
AISI 304 SUBSTRATE	93.4[a]	130.6[a]	7.5[a]
AISI 304 25 °C	82.2[b,c,d]	155.5[b]	4.7[b]
AISI 304 40 °C	77.9[b,c]	152.3[b]	5.2[b]
AISI 430 SUBSTRATE	89.7[a,b]	134.9[a]	6.9[a]
AISI 430 25 °C	72.8[d]	184.6[c]	3.0[c]
AISI 430 40 °C	75.1[c,d]	175.1[c]	3.5[c]

it was not possible to isolate the influence of the substrate, with a Bückle's rule of 1/10 [21].

Junqueira et al. [6] proposed a direct relationship of porosity (nm) with hardness when evaluating the properties of interference films grown on AISI 304 substrate under different process conditions, in golden color, since that interference films with larger pore diameter (higher porosity) presented lower hardness and larger deformation. The results found in this study are in consonance with those presented by the previous study.

3.2.4. *Wettability of interference films*

The wettability of the films in relation to water and oil was evaluated. Figure 5 shows the variation of the angle of contact of the water droplet with the surface of the substrate and films. It can be verified an increase of the hydrophilicity of the surface with the coloring process, which is more pronounced for the film grown on the AISI 430 SS substrate (see Fig. 6).

The influence of the coloring temperature can also be observed, with an increase in the contact angle as the coloring temperature increases. For the AISI 304 specimens, the same effect of the increase in wettability occurred after the coloring process, but the influence of the coloring temperature does not occur so sharply and directly since the colored samples at 35 °C and 40 °C were considered statistically identical.

When evaluating the angle of contact of the surface with oil, we verified that the surfaces of SS substrates are oleophilic, and become even more oleophilic after the coloring process, being not feasible even the measurement of the contact angle in oil, occurring an almost complete spread of the oil on the colored surface, as recorded in Table 4.

The effect of roughness on the amplification of wettability of heterogeneous and rough real surfaces of the Wenzel and Cassie-Baxter models can be confirmed by comparing it with the results of the nanoroughness test. The increase in the nanoroughness of the colored surface of AISI 430 and 304 steel produced an amplification of the hydrophilic effect of the surface. Kubiak et al. [15] studied the influence of roughness on the contact angle of different surfaces and confirmed the strong influence of roughness on the wettability of different engineering surfaces, with similar behaviors. Although the high standard deviation mainly for the AISI 304 steel, the effect of roughness on the wettability was identified and the results agree with the literature [14]. A higher roughness produced by the coloring process accentuated the hydrophilic character of the surface. This higher roughness could be of great value for surface modification with coatings such as Organically Modified Silicates, ORMOSIL [12], for example, providing a thin and transparent film on the colored surface, which could generate hydrophobic, oleophobic or amphiphobic surfaces on colored stainless steel.

By evaluating water wettability, we are predominantly evaluating the polar interaction of the surface, as well as when evaluating the wetness to the oil used. We evaluated the nonpolar interactions of the oil with the surface, that is, the affinity of coatings with liquids that have O–H (polar) or C–H (non-polar) connections [16]. Considering that for both liquids, water and oil, there was an increase in wettability after the coloring process, the polarity of the liquid did not affect the wettability in this case.

Further investigation will be necessary to increase the hydrophobicity and oleofibicity of colored stainless steel to obtain anti-finger prints or easy cleanings surfaces convenient for architectural applications.

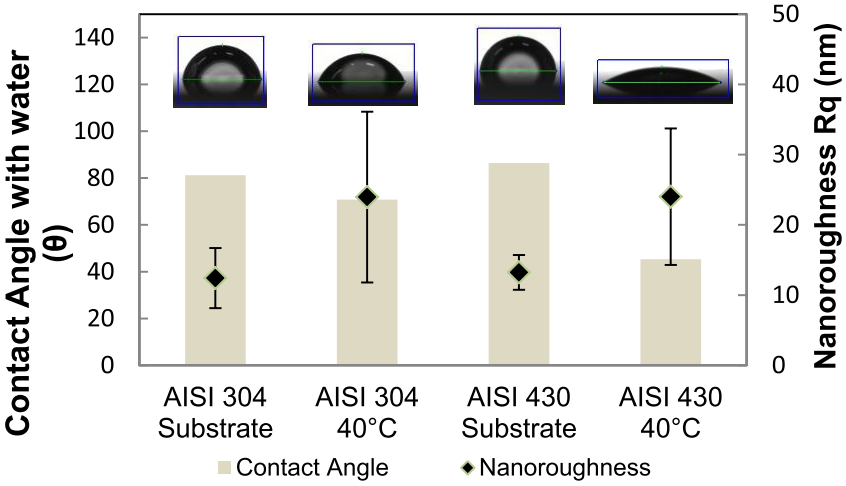

Fig. 6 – Mean values of the water contact angle and the mean quadratic roughness (Rq) obtained by AFM for substrates and colored samples at different temperatures.

Table 4 – Contact angles measured between the surface of the samples studied and a drop of oil, and images taken during the measurement.

	AISI 304 SS	AISI 304 25 °C	AISI 304 30 °C	AISI 304 40 °C
Contact Angle (θ)	14.2 ± 2.4	n.d.	n.d.	n.d.
				
	AISI 430 SS	**AISI 430 25 °C**	**AISI 430 30 °C**	**AISI 430 40 °C**
Contact Angle (θ)	10.0 ± 0.4	8.0 ± 1.5	n.d.	n.d.
				

Note: N.D. means "not detected", *i.e.* contact angle close to zero.

4. Conclusions

It was possible to color the AISI 304 and AISI 430 SS by an electrochemical process of pulsed current coloring, conferring to AISI 304 steel a higher growth rate of the interference film when compared to AISI 430 at the same process temperature. The temperature influenced the coloring process, with an exponential reduction of coloring time as the temperature increases.

The temperature influenced the properties of the nanofilms less than the substrate under which the interference film was generated. The pore size is larger for the interference films on the ferritic substrate. The nanoroughness of the films obtained by AFM showed more significant heterogeneity of the surface after coloring. It is not possible to affirm that there is a difference in nanoroughness influenced by the type of substrate. The nanohardness of the film–substrate conjugate decreased after the coloring process, and this reduction was more noticeable for the films on the ferritic substrate, possibly influenced by the larger pore size of these films. The values of the nanomechanical parameters evaluated were independent of the coloring process temperature. The wettability of the interference film surface to water and oil increases after the coloring process but, to water, it decreases with the increase of the coloration process temperature.

AISI 430 ferritic steel can be colored in golden with optimal conditions of 40 °C and time of 950 s, generating higher water contact angle and better mechanical properties in terms of elastic modulus and nanohardness among the studied conditions.

Declaration of Competing Interest

The authors declare that they have no known competing financial interests or personal relationships that could have appeared to influence the work reported in this paper.

Acknowledgments

The authors would like to thank APERAM South America and Inoxcolor for providing the samples, analysis, and reagents; UFMG Microscopy Center for the AFM and SEM images; Department of Metallurgical and Materials Engineering of UFMG for the use of the goniometer for the wettability measurements. We thank the financial support from PRPq-UFMG (03/2021).

REFERENCES

[1] Ji K, Xue Y, Cui Z. A new method for colors characterization of colored stainless steel using CIE and Munsell color systems. Opt Mater 2015;47:180–4. https://doi.org/10.1016/j.optmat.2015.05.014.

[2] Conrrado R, Bocchi N, Rocha-Filho RC, Biaggio SR. Corrosion resistance of colored films grown on stainless steel by the alternating potential pulse method. Eletrochim. Acta. 2003;48:2417–24. https://doi.org/10.1590/S0103-50532004000400005.

[3] Kikuti E, Conrrado R, Bocchi N, Biaggio SR, Rocha-Filho RC. Chemical and electrochemical coloration of stainless steel and pitting corrosion resistance studies. J Braz Chem Soc 2004;15:472–80. https://doi.org/10.1590/S0103-50532004000400005.

[4] Evans TE. Film formation on stainless steel in a solution containing chromic and sulphuric acids. Corrosion Sci 1977;17:105–24. https://doi.org/10.1016/0010-938X(77)90012-9.

[5] Fujimoto S, Tsujino K, Shibata T. Growth and properties of Cr-rich thick and porous oxide films on type 304 stainless steel formed by square wave potential polarisation. Electrochim Acta 2001;47:543–51. https://doi.org/10.1590/s1517-707620170001.0323.

[6] Junqueira RMR, Loureiro CRO, Andrade MS, Buono VTL. Mechanical properties of interference thin films on colored stainless steel evaluated by depth-sensing nanoindentation. Surf Coating Technol 2006;201:2431–7. https://doi.org/10.1590/S1516-14392008000400007.

[7] Wang JH, Duh JG. Colour tone and chromaticity in a colored film on stainless stel by alternating current eletrolysis method. Surf Coating Technol 1995;73:46–51. https://doi.org/10.1016/0257-8972(94)02359-X.
[8] Junqueira RMR, Manfridini APA, Loureiro CRO, Mendonca R, Macedo WAA. Morphological, chemical and mechanical characteristics of an anodic coating on stainless steel. Surf Eng 2013;29:379–83. https://doi.org/10.1179/1743294413Y.0000000126.
[9] Fogler HS. Essentials of chemical reaction engineering. 4th ed. Rio de Janeiro: LTC; 2009.
[10] Corredor J, Bergmannb CP, Pereira M, Dick LFP. Coloring ferritic stainless steel by an electrochemical–photochemical process under visible light illumination. Surf Coating Technol 2014;245:125–32. https://doi.org/10.1016/j.surfcoat.2014.02.051.
[11] Qu J-e, Yu C, Cui R, Qin J, Wang H, Cao Z. Preparation of super-hydrophobic and corrosion resistant colored films on chemically etched 304 stainless steel substrate. Surf Coating Technol 2018;354:236–45. https://doi.org/10.1016/j.surfcoat.2018.09.022.
[12] Carneiro ARC, Ferreira FAS, Houmard M. Easy functionalization process applied to develop super-hydrofobic and oleophobic properties on ASTM 1200 aluminum surface. Surf Interface Anal 2018;50:1–14. https://doi.org/10.1002/sia.6532.
[13] Su MJ, et al. Controllable wettability on stainless steel substrates with highly stable coatings. Chem Eng Sci 2019;195:791–800. https://doi.org/10.1016/j.ces.2018.10.025.
[14] Butt H, Graf K, Kappl M. Physics and chemistry of interfaces. Darmstadt: Wiley-VCH Verlag & Co; 2003.
[15] Kubiak KJ, Wilson MCT, Mathia TG, Carval P. Wettability versus roughness of engineering surfaces. Wear 2011;271:523–8. https://doi.org/10.1016/j.wear.2010.03.029.
[16] Houmard M, Vasconcelos DCL, Vasconcelos WL, Berthomé G, Joud JC, Langlet M. Water and oil wettability of hybrid organic–inorganic titanate–silicate thin films deposited via a sol–gel route. Surf Sci 2009;603:2698–707. https://doi.org/10.1016/j.susc.2009.07.005.
[17] CETEC. Minas GeraisTechnological Foundation Center. Electrochemical coloration process of stainless steel. 1999.
[18] IMAGEJ- image processing and analysis in java. Versão 1.8.0_112, https://imagej.nih.gov/ij/download.html. [Accessed 3 January 2020].
[19] PAST: paleontological statistics software package for education and data analysis. Hammer & Harper; 2020. Versão: 2.17, http://priede.bf.lu.lv/ftp/pub/TIS/datu_analiize/PAST/2.17c/download.html. [Accessed 1 February 2020].
[20] Callister WD. Materials science and engineering: an introduction. 5th ed. Rio de Janeiro: LTC; 2002.
[21] Oliver WC, Pharr GM. An improved technique for determining hardness and elastic modulus using load and displacement sensing indentation experiments. J Mater Res 1992;7:1564–83. https://doi.org/10.1557/JMR.1992.1564.